Optik - International Journal for Light and Electron Optics 251 (2022) 168139

Contents lists available at ScienceDirect

Optik - International Journal for Light and Electron Optics

journal homepage: www.elsevier.com/locate/ijleo

Original Research Article

Calculation of conic constants for thick lenses to get diffraction-limited images using 3rd order design and marginal skew ray tracing

F. Narea-Jiménez [a,b,*], J. Castro-Ramos [a], J.J. Sánchez-Escobar [c], Ma.T. Chávez-García [d], A. Vázquez-Villa [e], G. Silva-Ortigoza [f]

[a] Optica, Instituto Nacional de Astrofísica Óptica y Electrónica, Puebla, C.P. 72001, Puebla, Mexico
[b] Departamento de Física, Facultad Experimental de Ciencias y Tecnología, Universidad de Carabobo, Valencia, C.P. 2005, Carabobo, Venezuela
[c] Centro de Enseñanza Técnica Industrial, Nueva Escocia 1885, Fraccionamiento Providencia 5a Sección, C.P. 44638, Guadalajara, Mexico
[d] Universidad Politécnica de Tlaxcala, Programa Educativo Ing. Industrial, C.P. 90180, Tlaxcala, Mexico
[e] Division of Advanced Materials, Instituto Potosino de Investigación Científica y Tecnológica (IPICYT), C.P. 78216, San Luis Potosí, Mexico
[f] Benemérita Universidad Autónoma de Puebla Postgrado en Opto electrónica, Apdo. Postal 51 y 217, C.P. 72000, Puebla, Mexico

ARTICLE INFO

Keywords:
Optical design
Thick lenses
Spherical aberration
Coma aberration
Conics surfaces
Diffraction limit

ABSTRACT

We calculate equations to obtain the exact and third-order design of thick lenses free from spherical and coma aberrations at two points, at the edge and center of the lens, considering the shape factor and the conic constants. We obtained analytical expressions based on the equality of the optical path and the Abbe sine condition calculated for an object located in infinite and finite positions. Examples developed with this method show an alternative way of designing diffraction-limited thick lenses that are equal or better than results obtained when the conic constants are optimized using commercial optical design software. As the shape of the lens changes, the spherical and coma aberrations vary; so, the presented method offers better results for shape factors ranging from −0.5 to 0.9.

1. Introduction

The most used optical systems today are lenses, as they allow the formation of images and have the ability to concentrate light coming from a lighting source inside and outside the optical axis.

As optical elements, lenses by nature of their surfaces introduce aberrations into the image. If the surfaces are spherical, spherical aberration occurs; however, if the object is at infinity or is finite, outside the optical axis, coma aberration occurs. The field of view of the lens affects aberrations due to the differences in the optical path length between the marginal and paraxial rays. Therefore, the properties and applications of lenses have been studied from long ago to the present. Some studies show that these aberrations reduce by different shape factors and the conjugate variable [1–3]. Castro et al. [4] have developed an analytical method that allows a spherical singlet to be modified by another non-spherical curved surface to minimize spherical aberration of infinite and finite conjugate objects.

In the literature, we find that Jurek [5] developed a numerical evaluation to design an aplanatic lens using a differential equation and determine the relationships between the Cartesian coordinates of the meridian plane and the second surface using the equal optical path theorem.

* Corresponding author at: Optica, Instituto Nacional de Astrofísica Óptica y Electrónica, Puebla, C.P. 72001, Puebla, Mexico.
E-mail addresses: fjnarea@inaoep.mx, fjnarea@uc.edu.ve (F. Narea-Jiménez).

https://doi.org/10.1016/j.ijleo.2021.168139
Received 22 March 2021; Received in revised form 17 August 2021; Accepted 8 October 2021
Available online 27 November 2021

Máximo Avendaño and collaborators [6] presented another all-important aspect of singlets; they studied the formation of the caustic surface produced by conics lenses thick considering a flat wavefront to create sharper diffraction-limited images (to reduce third-order spherical aberration). Alternatively, the caustic surface made in a large area can be applied to singlets' design without imaging, with potential applications such as diffusers for lighting or solar concentrators.

Chaohsien Chen [7] highlighted the importance of studying variations in spherical and coma aberrations in singlets. Some authors [8] reveal interest in diffraction lenses. In this case, a singlet diffractive optical element provides the possibility of correcting aplanatism. The combination of lenses with spherical surfaces and diffractive optical elements is difficult to construct when the spatial frequency is considerable.

Another essential application concerning the use of singlets is presented by Mingqian Zhang [9]. The proposed work is to design a coherent light collimator using a fiber-optic arrangement consisting mainly of a single collimation lens. The distribution of the far-field intensity pattern detected by an infrared camera matches the ideal intensity distribution.

Using the Abbe sine condition for performing optical designs, Masato Shibuya [10] established that spherical aberration can exist without coma aberration and conventional aberration theory is reliable in the third-order region.

Rafael González et al. [11] presented exact equations to design a stigmatic singlet on the axis, satisfying the Abbe sine condition for each ray-traced over the entire surface. They solve a nonlinear system to find a function describing the second surface, previously fixing the first surface as a parabola. The function they find represents a challenge for optical shops in charge of the construction of refractive optical surfaces.

Mikš and Pokorný [12] developed a theoretical analysis of a rotationally symmetric lens system's characteristics, with one or two aspheric surfaces, to produce a stigmatic system mainly on axis from the Seidel sums. These articles highlight the importance of solving this problem, which has been addressed for several decades, for example, in the 1980s by Born and Wolf [13] where he presents a treatment with a system of two differential equations, which maps the points of the aspheric surfaces for the particular cases when the object or image is at infinity.

Even though optical systems consist of several lenses, an aplanatic singlet designed with two surfaces helps evaluate skin lesions using monochromatic light. It allows the extraction of lesion characteristics in a specific spectral analysis; furthermore, it is also helpful in designing contact and intraocular lenses to analyze wavefront aberration, as Srivastava et al. showed [14].

An important aspect to highlight is that computational tools optimize calculations to perform aberration-free optical systems. Sometimes the third-order design has been used as a starting point to perform up optical designs. Based on the concepts and theories developed in a previously published article [4]. We propose a singlet design with conic surfaces free of spherical and coma aberrations by computing aberrations' correction at two points at the lens's edge and center. Thus, we showed that only any two points on the lens surfaces are sufficient to find a diffraction-limited system. Optical thick lens designs start from third-order, subsequently by using exact ray tracing. This method applies to both near and far objects with monochromatic light.

2. Reduction of spherical and coma aberrations by using first and third order design

This section describes how any thick lens optical design starts (see Fig. 1). First of all, by calculating the thin lens parameters, the focal length of the lens f, its inverse refractive power ϕ ($\phi = 1/f$), and the image position (d_2). In the second place, by computing parameters such as the distance between the thick lens's vertex and the object's position (d_0), the radii of curvature (r), the shape factor (B), the refractive index (n'), and the conjugate factor ($C = -\left(1 + \frac{2f}{d_0}\right)$) [4].

2.1. Thin lens

Castro et al. [4] deduced the radii of curvature of the first and second surfaces for a thin lens with minimal spherical aberration. With an analogous procedure using Seidel sums [15], Welford has shown that the best shape factor must obtain for finding a minimal coma aberration utilizing the equation:

$$B = -\frac{(n'-1)(2n'+1)}{n'+1}C. \tag{1}$$

By substituting the shape factor ($B = \frac{(r_2+r_1)}{(r_2-r_1)}$) into Eq. (1), it is possible to find the radius of curvature of the first and second surfaces for a lens that reduces coma aberration:

$$r_i = \frac{2f(n'^2-1)}{(n'-1)(2n'+1)\left(1+\frac{2f}{d_0}\right) \pm (n'+1)}, \tag{2}$$

combining Eqs. (1) and (2), we obtain the curvature radius in terms of the shape factor B:

$$r_i = \frac{2f(n'-1)}{B \pm 1}, \tag{3}$$

the positive sign uses when the subscript $i = 1$, and for $i = 2$, we must apply the negative sign of the Eq. (3).

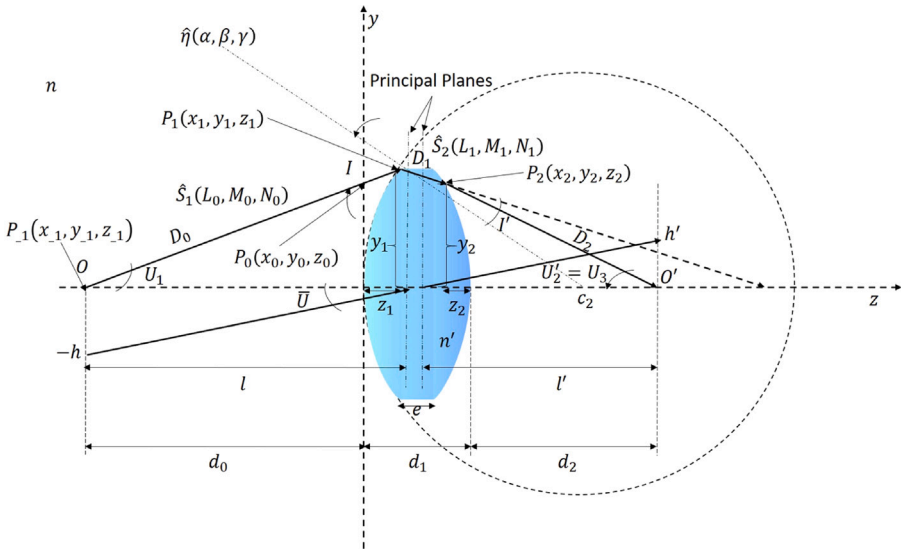

Fig. 1. Design parameters of a singlet in a meridional plane for an inside and outside the optical axis object point (O).

2.2. Thick lens

In reality, in an optical system, lenses have an axial thickness

$$d_1 = e + z_1 - z_2, \tag{4}$$

where e is the lens edge thickness. The sagittas (z_1, z_2) are functions of the conic constants of the surfaces k_i, the incidence height of the ray concerning the optical axis y_i, and the vertex of the lens [16].

$$z_i = \frac{c_i y_i^2}{1 + \sqrt{1 - (k_i + 1)c_i^2 y_i^2}} \qquad i = 1, 2. \tag{5}$$

If at the beginning of the design this considers a spherical surface ($k_i = 0$), then to obtain real values of Eq. (5) of the sagitta z, then it requires $1 - c_i^2 y_i^2 \geq 0$ must be satisfied. Therefore, the curvature c_i of the lens must meet the condition given by Eq. (6):

$$c_i \leq \frac{2f\text{-number}}{f} \qquad i = 1, 2. \tag{6}$$

According to Castro et al. [4], Eq. (7) calculates the curvature radii for a thick lens without changing the original design's paraxial focal length.

$$r_i = (n' - 1)\frac{f + [f^2 + (f d_1/n')(B + 1)(B - 1)]^{1/2}}{B \pm 1}, \tag{7}$$

where the positive sign is used for $i = 1$ and the negative sign for $i = 2$, hence, using the Eq. (5) to (7), we obtain the first-order parameters necessary to design a thick lens with effective focal length f, the axial thickness d_1, and refractive index n'.

In general, a third-order analysis may be enough to obtain the final optical design of various instruments. This fact achieved by correcting and eliminating aberrations to improve image quality, by working with the Seidel aberrations, and the conic constants of aspherical surfaces, as is shown in the next section.

2.3. Optical design to third-order with aspherical surfaces

In this section, the third-order conic constants calculate for any thin lens, thus obtaining a system free of spherical aberration. It is well known that the total deformation of the wavefront must consist of the contributions introduced by a conic surface of revolution plus the aberration produced by the spherical reference surface as follows:

$$SI_{total} = SI_{spherical} + SI_{conic}, \tag{8}$$

where $SI_{spherical}$ is the first Seidel sum for spherical surfaces [2,15,17] and SI_{conic} is the contribution of the conic surface given by Shannon [17].

$$SI_{spherical} = \sum_{i=1}^{K} y_i (n_i n_{i+1})^2 \left(\frac{U_{i+1} - U_i}{n_{i+1} - n_i}\right)^2 \left(\frac{U_{i+1}}{n_{i+1}} - \frac{U_i}{n_i}\right), \tag{9a}$$

$$SI_{conic} = \mp \left(n' - 1\right) k_i c_i^3 y_i^4, \tag{9b}$$

where (U_{i+1}, U_i) are the angles formed by the marginal ray path, and the optical axis, (n_{i+1}, n_i) are the refractive indices, k_i is the conic constant, and $c_i = 1/r_i$ is the curvature. The subscripts $i = 1, 2$ in the Eq. (9b) refer to the first surface (negative sign) and the second surface (positive sign), respectively, and y_i is the height of the marginal ray.

Expanding Eq. (9a) for $K = 2$, where $n_{i+1}U_{i+1} = n_iU_i + y_i(n_{i+1} - n_i)/r_i$, $y_{i+1} = y_i - d_iU_{i+1}$, $n_1 = n_3 = 1$ and $n_2 = n'$, we get

$$\begin{aligned} SI_{spherical} = \frac{y_1^4}{n'^2(n'-1)^2} \Bigg\{ & (\mathcal{J}_1 - \frac{n'}{d_0})^2(\mathcal{J}_1 - \frac{n'^2}{d_0}) + \frac{\mathcal{O}_1}{n'(B-1)^3} \\ & \left[\mathcal{J}_1(B-1)(n'-1) - (B+1)\phi_1\mathcal{O}_1\right]^2 \\ & \left[\mathcal{J}_1(n'^2-1)(B-1) - (B+1)\phi_1 n'\mathcal{O}_1\right] \Bigg\}, \end{aligned} \tag{10}$$

where $\mathcal{O}_1 = n' - d_1\mathcal{J}_1$, $\mathcal{J}_1 = 1/d_0 + \phi_1$ and $\phi_1 = (n'-1)/r_1$. If the object is at infinity ($d_0 = \infty$), $y_1 = 1$, and the focal length is 1, Eq. (10) reduces to Mikš's [18,19] equation for Seidel spherical aberration for a thick lens in air.

Now from Eqs. (8), (9b), and (10), the conic constants k_i for a minimum contribution of spherical aberration of any thick lens are calculated by:

$$\begin{aligned} k_1 = \frac{\phi_1^{-3}}{n'^2} \Bigg\{ & (\mathcal{J}_1 - \frac{n'}{d_0})^2(\mathcal{J}_1 - \frac{n'^2}{d_0}) + \frac{\mathcal{O}_1}{n'(B-1)^3} \left[\mathcal{J}_1(B-1)(n'-1)\right. \\ & \left. -(B+1)\phi_1\mathcal{O}_1\right]^2 \left[\mathcal{J}_1(n'^2-1)(B-1) - (B+1)\phi_1 n'\mathcal{O}_1\right] \Bigg\}, \end{aligned} \tag{11a}$$

$$\begin{aligned} k_2 = -\frac{(B+1)^3\phi_1^{-3}}{n'^2(B-1)^3(1-\frac{d_1}{n'}\mathcal{J}_1)^4} \Bigg\{ & (\mathcal{J}_1 - \frac{n'}{d_0})^2(\mathcal{J}_1 - \frac{n'^2}{d_0}) \\ & + \frac{\mathcal{O}_1}{n'(B-1)^3}\left[\mathcal{J}_1(B-1)(n'-1) - (B+1)\phi_1\mathcal{O}_1\right]^2 \\ & \left[\mathcal{J}_1(n'^2-1)(B-1) - (B+1)\phi_1 n'\mathcal{O}_1\right] \Bigg\}. \end{aligned} \tag{11b}$$

These equations allow computing a lens designed with minimal third-order aberrations, with conic constants calculated from the Seidel equations.

The third-order conic constants were calculated to minimize spherical aberrations and coma. Still, if the lenses have f-number < 5, and the field angle is large, the optical designs equations computed render non-tolerable aberrations. When the focal ratio is less than 5, the third-order aberrations are considerable and inadequate to consider a final optical design with this methodology. Traditionally, it is possible to design optical systems by making computations through successive approximations of third, fifth, and seventh order for the wavefront aberration coefficients. We prefer to make corrections using the exact ray trace to reduce spherical and coma aberrations at the center and the aperture edge of the lens.

The following section explains a method to correct spherical and coma aberrations for thick lenses designed using exact ray tracing, which improves the computations of the third-order.

3. Reduction of spherical aberration and coma of a singlet, far object $d_0 = \infty$, exact ray tracing case

In this section of the article, to reduce spherical aberration, the condition used that both the paraxial optical path $\mathcal{L}_1$ and the length of the marginal optical path $\mathcal{L}_2$ should be the same [4]. Knowing the initial coordinates (x_1, y_1, z_1) and the director cosines of the incident ray $\hat{S}_1 = (L_0, M_0, N_0)$ on the first surface of the lens (see Fig. 1), we can know the direction of the refracted ray by the first surface $\hat{S}_2 = (L_1, M_1, N_1)$ using the method of transfer between conic surfaces [15].

Castro et al. [4] found the coordinates of the point $P_2(x_2, y_2, z_2)$ to determine the conic constant of the second surface using the general equation:

$$k_i = \frac{2z_i - c_i(y_i^2 + z_i^2)}{c_i z_i^2} \qquad i = 1, 2, \tag{12}$$

where the coordinates y_2 and z_2 are given by

$$y_2 = y_1 + M_1 D_1, \tag{13a}$$

$$z_2 = z_1 - d_1 + N_1 D_1 \tag{13b}$$

which are functions that depend on the parameter D_1 represented in Fig. 1, M_1 and N_1 are the director cosines of the refracted ray on the first surface, and D_1 shall obtain by solving the quadratic equation:

$$(1 - n'^2)D_1^2 + 2[y_1M_1 - (d_2 - z_1 + d_1)N_1 + (n'd_1 + d_2 - z_1)n']D_1$$

$$+ [y_1^2 + (d_2 - z_1 + d_1)^2 - (n'd_1 + d_2 - z_1)^2] = 0. \tag{14}$$

Castro et al. [4] derived the above equation. Whether both the discriminant ≥ 0 and the quadratic equation satisfies Eq. (5), we obtain the real solution to the Eq. (14). Hence, the correct answer must be the one with a positive sign. We find the conic constant's value that corrects exact spherical aberration for a thick lens with this solution.

One goal of this paper is to design aplanatic lenses, hence, coma aberration must be eliminated simultaneously with the spherical one; therefore, Section 3.1 presents the development to find the exact equations that correct coma aberration.

3.1. Equations to correct coma aberration

As Kingslake remarked [2], if f_p is the distance from the second principal plane to the focal point measured along any paraxial ray, and if F_m is the focal distance to any marginal ray such that:

$$F_m = \frac{y_1}{\sin U_3}, \tag{15}$$

then to get a thick lens free of coma aberration, the Abbe Sine condition must be satisfied, which means that $F_m = f_p$ and

$$f_p = \frac{y_1}{\sin U_3}. \tag{16}$$

From Fig. 1, we get

$$\sin U_2 = -\frac{y_2}{D_2}. \tag{17}$$

Substituting Eq. (17) into (16), we find that:

$$f_p = -\frac{y_1}{y_2} D_2. \tag{18}$$

Substituting the distance $D_2 = \sqrt{y_2^2 + (d_2 - z_2)^2}$ computed along the marginal ray into Eq. (18):

$$-\frac{y_2 f}{y_1} = \sqrt{y_2^2 + (d_2 - z_2)^2}. \tag{19}$$

This equation is squared and substituting into it the coordinates of the point $P_2(y_2$ and $z_2)$ given by the Eq. (13a) and Eq. (13b), to get :

$$(y_1 + M_1 D_1)^2 (f^2 - y_1^2) = y_1^2 (d_2 - (z_1 - d_1 + N_1 D_1))^2. \tag{20}$$

By expanding and making algebra in Eq. (20), a second-degree equation obtains in variable D_1, given by:

$$\left(M_1^2 f_p^2 - y_1^2\right) D_1^2 + 2y_1 \left[M_1 \left(f_p^2 - y_1^2\right) + y_1 \left(d_2 + d_1 - z_1\right) N_1\right] D_1 + y_1^2 \left[f_p^2 - y_1^2 - (d_2 + d_1 - z_1)^2\right] = 0. \tag{21}$$

Now substituting Eq. (21) into (14), we obtain a fourth-degree equation in variable z_1, given by:

$$\left\{ \frac{-2\left[y_1 M_1 - (d_2 - z_1 + d_1) N_1 + (n'd_1 + d_2 - z_1) n'\right]}{2(1 - n'^2)} + \frac{1}{(2(1-n'^2))} \left[\begin{array}{c} 2\left[y_1 M_1 - (d_2 + d_1 - z_1) N_1 + (n'd_1 + d_2 - z_1) n'\right]^2 - \\ 4(1 - n'^2)\left[y_1^2 + (d_2 + d_1 - z_1)^2 - (n'd_1 + d_2 - z_1)^2\right] \end{array} \right]^{1/2} \right\}^2 +$$
$$2y_1 \left[(f^2 - y_1^2) M_1 + y_1 (d_2 - z_1 + d_1) N_1\right] \cdot$$
$$\cdot \left\{ \frac{-2\left[y_1 M_1 - (d_2 - z_1 + d_1) N_1 + (n'd_1 + d_2 - z_1) n'\right]}{2(1 - n'^2)} + \frac{1}{(2(1-n'^2))} \left[\begin{array}{c} 2\left[y_1 M_1 - (d_2 + d_1 - z_1) N_1 + (n'd_1 + d_2 - z_1) n'\right]^2 - \\ 4(1 - n'^2)\left[y_1^2 + (d_2 + d_1 - z_1)^2 - (n'd_1 + d_2 - z_1)^2\right] \end{array} \right]^{1/2} \right\} +$$
$$y_1^2 \left[f^2 - y_1^2 - (d_2 - z_1 + d_1)^2\right] = 0. \tag{22}$$

The director cosines L_1, N_1 and M_1 depend on z_1; hence the Eq. (22) ensures that we have a system free of spherical and coma aberration; it is an exact equation that makes no approximations during its derivation. For practical purposes, the Eq. (22) can be solved numerically using a root search method, e.g., the Newton–Raphson method for a non-linear equations system.

Four solutions for z_1 are obtained that satisfy the Eq. (22), but the only one that allows the correct solution of the conic surface depends on the following considerations: If the curvature radius c_1 is positive, then $z_1 > 0$. If c_1 is negative, then $z_1 < 0$. Hence the coordinate (y_1, z_1) must locate on the periphery of a conic section near the vertex-object of the initial spherical surface (see Fig. 2).

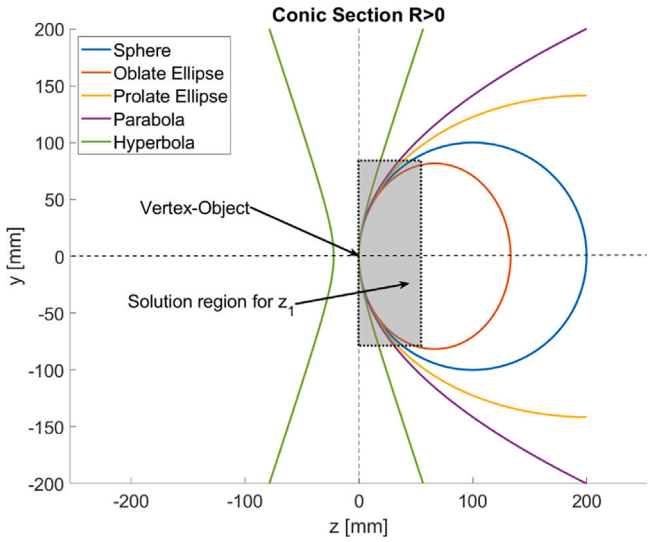

Fig. 2. Representation of the selected, correct solution for z_1. The gray rectangle represents the region of solutions z_1 that satisfies our aplanatic system's conditions without inverting the surfaces' curvature.

Once the correct solution for z_1 is selected, the Eq. (22) is substituted into Eqs. (12) and (21) to obtain the value of the conic constant of the first surface k_1 and parameter D_1, respectively. With D_1, the coordinate $(y_2; z_2)$ is determined to be substituted into Eq. (12) for finding the conic constant of the second surface (k_2). With that, we guarantee thick lens aberrations are corrected both at the focal point and at one height of the optical axis of the incident ray. The above description is sufficient to design diffraction-limited lenses with exact ray tracing for an object at infinity.

An object at infinity is not the only position used in optical instruments; for example, a close object to the lens uses in the microscope's design. The following section shows how to design a thick lens for near objects to the optical system.

4. Singlet lens with reduction of spherical and coma aberrations, near object, accurate ray trace case

Following the methodology developed in the previous section, the object's finite position equations are calculated to obtain a diffraction limit lens.

In this case, it is necessary to know the first-order parameters obtained, as mentioned in Section 2. Besides, the refractive index n', the magnification m, the object position d_0, and the f-number, parameters provided in Section 2 (see Fig. 1). Additionally, the paraxial and marginal rays' optical paths must be equal to obtain a singlet lens free of spherical aberration [4].

$$(1-n'^2)D_1^2 + 2[(d_0 + n'd_1 + d_2 - D_0)n' + y_1 M_1 - (d_2 + d_1 - z_1)N_1]D_1 + [y_1^2 + (d_2 + d_1 - z_1)^2 - (d_0 + n'd_1 + d_2 - D_0)^2] = 0. \tag{23}$$

Castro et al. [4] details the development of Eq. (23) to correct spherical aberration.

4.1. Correction of coma aberration

Abbe [20–23] established a ratio for coma aberration as a difference in heights from one image to another on each surface of an optical system. Furthermore, he deduced that a spherical aberration-corrected optical system could be free of coma aberration if the paraxial magnification m and the marginal magnification M are equal. Hence:

$$m = M = \frac{\sin U_1}{\sin U_3}. \tag{24}$$

From Fig. 1, it is easy to obtain something like:

$$\sin U_1 = \frac{y_1}{D_0}, \tag{25a}$$

$$\sin U_3 = -\frac{y_2}{D_2}. \tag{25b}$$

Combining the Eqs. (25a), (25b), the distance along the marginal ray D_2, coordinates z_2 and y_2, and after performing some algebraic operations, it is possible to obtain a second-degree equation for D_1.

$$(m^2 D_0^2 M_1^2 - y_1^2)D_1^2 + 2y_1\left[(m^2 D_0^2 - y_1^2)M_1 + (d_2 + d_1 - z_1)N_1 y_1\right] D_1$$

Table 1
Optical parameters of a lens with a focal length equal to 60 mm and $f/2.5$.

	Radius [mm]	Thickness [mm]	Index Glass	Semi Diameter [mm]	Conic
Obj.	∞	∞	1	∞	0
Surf.1	33.7805	3.7013	1.5168	12	−0.5318
Surf.2	−363.6379	57.7605	1	12	−272.0541
Img.	∞	0	1	0	0

$$+ y_1^2\left[m^2D_0^2 - y_1^2 - (d_2 + d_1 - z_1)^2\right] = 0. \tag{26}$$

Eq. (26) gives us a condition to obtain an optical system free of coma aberration while the optical system is free of spherical aberration.

Substituting Eq. (23) into (26), a fourth-degree equation is obtained for z_1:

$$\begin{aligned}
&(m^2D_0^2M_1^2 - y_1^2)\\
&\left\{\begin{array}{c}\frac{-2\left[y_1M_1-(d_2-z_1+d_1)N_1+(n'd_1+d_2-d_0-D_0)n'\right]}{2(1-n'^2)}+\\ \frac{1}{(2(1-n'^2))}\left[\begin{array}{c}2\left[y_1M_1-(d_2+d_1-z_1)N_1+(n'd_1+d_2-d_0-D_0)n'\right]^2-\\ 4(1-n'^2)\left[y_1^2+(d_2+d_1-z_1)^2-(n'd_1+d_2-d_0-D_0)^2\right]\end{array}\right]^{1/2}\end{array}\right\}+\\
&2y_1\left[(m^2D_0 - y_1^2)M_1 + y_1(d_2 - z_1 + d_1)N_1\right]\cdot\\
&\cdot\left\{\begin{array}{c}\frac{-2\left[y_1M_1-(d_2-z_1+d_1)N_1+(n'd_1+d_2-d_0-D_0)n'\right]}{2(1-n'^2)}+\\ \frac{1}{(2(1-n'^2))}\left[\begin{array}{c}2\left[y_1M_1-(d_2+d_1-z_1)N_1+(n'd_1+d_2-d_0-D_0)n'\right]^2-\\ 4(1-n'^2)\left[y_1^2+(d_2+d_1-z_1)^2-(n'd_1+d_2-d_0-D_0)^2\right]\end{array}\right]^{1/2}\end{array}\right\}+\\
&y_1^2\left[m^2D_0^2 - y_1^2 - (d_2 - z_1 + d_1)^2\right] = 0.
\end{aligned} \tag{27}$$

With the methodology developed in Section 3 and with Eq. (27) deduced in this section, it is possible to calculate the conic constants, which allow the design of a thick singlet free of spherical and coma aberration for a near object at the diffraction limit. Thus, are corrected two incident rays, one the marginal and the other on the optical axis.

5. Examples

The developed method is essential for optical engineering because it solves the problem of finding the optimal optical design of a thick lens at the diffraction limit, which is very useful for several applications, as mentioned in the introduction. Equations obtained are implemented with a homemade algorithm executed in Matlab® R2020a for shape factors ranging from −0.5 to 0.9. The proposal validates with examples of thick lens designs. This algorithm is practical to design singlet both third-order and for exact order. Equations solve numerically, depending on either a wide lens with a far or near object is considered and with one or two conic surfaces.

One of the goals of designing an optical system is to optimize the design until the diffraction limit; the developed method has that capacity. As an example of this, two optical systems show next.

A first example shows one lens's design to reduce the most remarkable aberrations, with a focal length of 60 mm, the f-number of 2.5, a shape factor of 0.83, and two conic constants use to correct spherical and coma aberrations. Commercial glass BK7 from the Schott AG® catalog proposes for the visible region. The diameter of the lens is $D = f/f$-number= 24 mm. Using Eq. (3) we first determine the radii of curvature for a thin lens $r_1 = 33.8878$ mm and $r_2 = -364.7929$ mm, which we calculate the sagittas $z_1 = 2.1957$ mm and $z_2 = -0.1974$ mm using the Eq. (5), considering that initially the lens is made up of spherical surfaces ($k_1 = k_2 = 0$) and that the height $y_1 = y_2 = D/2 = 12$ mm. In an iterative process, the initial sagitta values and a lens edge thickness $e = 1.30$ mm in conjunction with the Eqs. (4), (5), and (7) allow to maintain the focal length [4], and an axial thickness is calculated $d_1 = 3.7013$ mm and radii of curvature for a thick lens $r_1 = 33.7805$ mm and $r_2 = -363.6379$ mm. The position of the image is equal to $d_2 = f + H_2 = 57.7605$ mm, where $H_2 = -2.2399$ mm is the position of the principal plane of the second surface [24].

In Table 1 are displayed the first-order parameters. We compute the four possible values of the sagitta z_1 to satisfy Eq. (22), from which it chose an estimation for $z_1 = 2.1638$ mm following the consideration for the curvature radius shown in Fig. 2, where the values of the new sagittas should not implicate a change in the curvature or the thickness of the lens. This value of z_1 allows calculating the director cosines of the refracted ray by the first surface $L_1 = 0$, $M_1 = -0.1220$, and $N_1 = 0.9925$ by using the transfer between conic surfaces, which are replaced in Eq. (21) to determine $D_1 = 1.3672$ mm which is used to calculate the coordinates $y_2 = 11.8331$ mm and $z_2 = -0.1804$ mm using the Eqs. (13a) and (13b) respectively. Finally, we calculate the conic constants for the first and second surfaces using Eq. (12), and these are equal to −0.5318 and −272.0541, respectively.

With these values, was possible to minimize spherical and coma aberrations for a thick lens. Using the optical design software ZEMAX®, we validate our equations developed in Sections 3 and 4 to design an optical system free of spherical aberration and coma

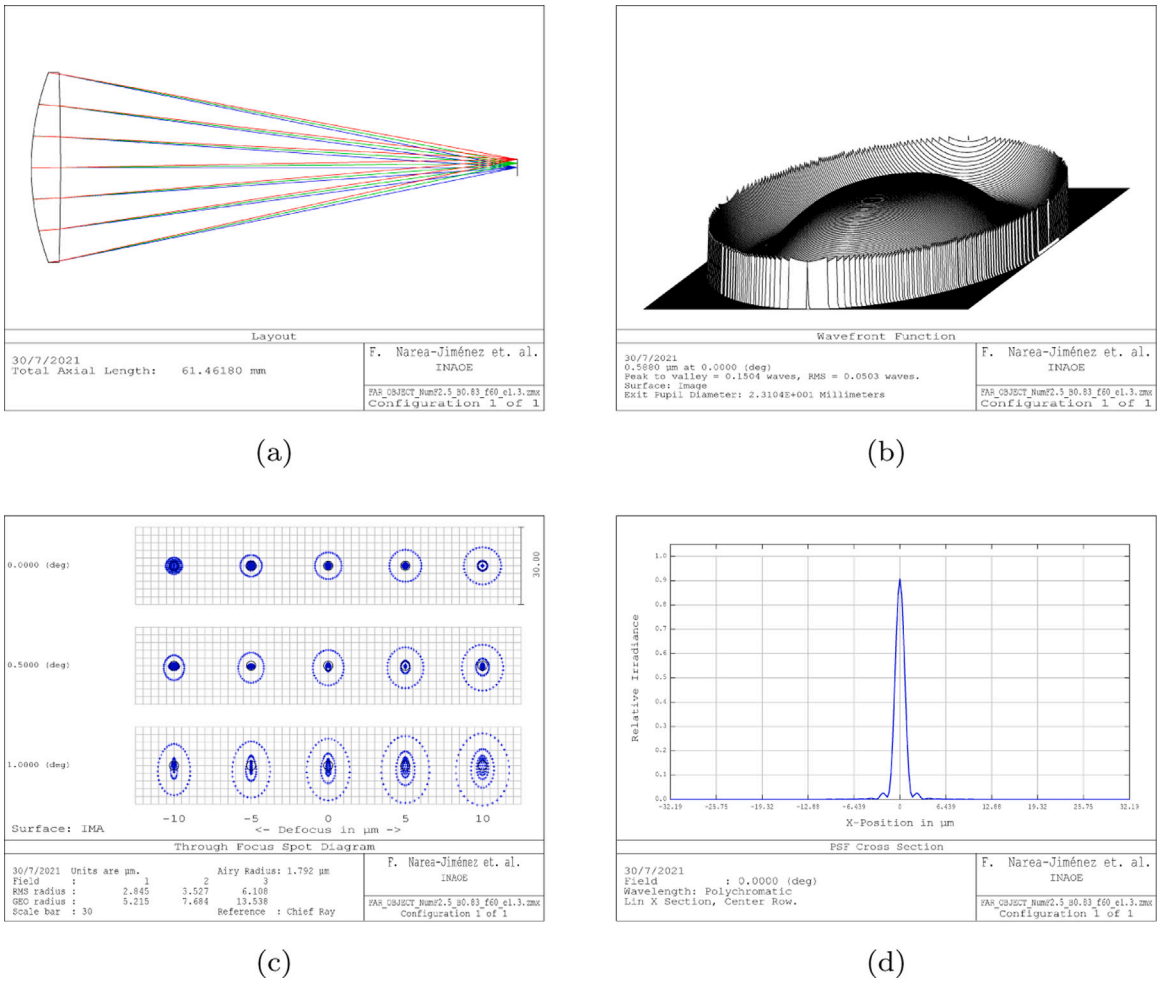

Fig. 3. Design case of an infinite conjugate singlet.

Table 2
Optical parameters of a lens with magnification equal to −3 and $f/2.5$.

	Radius [mm]	Thickness [mm]	Index Glass	Semi Diameter [mm]	Conic
Obj.	∞	56.3551	1	0	0
Surf.1	73.1455	7.8122	1.5168	9	−8.2255
Surf.2	−32.8624	178.3624	1	9	−1.0012
Img.	∞	0	1	0	0

aberration, the graphs in Figs. 3 and 4 warrantees that we have a diffraction-limited design. The use of this software allows us to show the goodness of this work's results. The first simulated example in ZEMAX® Fig. 3(a) shows a sketch of the designed lens. As can be seen, each incident ray converges to the same point. Fig. 3(b) shows the wavefront with a peak-to-valley value of 0.1596λ and the RMS wavefront error of 0.0529λ, $\lambda = 588$ nm. Fig. 3(c) shows that the lens exhibits residual spherical aberrations in the spot diagrams and does not show coma aberration; it shows an astigmatism spot diagram. Fig. 3(d) shows the PSF (Point Spread Function), which reveals a Strehl ratio of 0.8968, confirming a diffraction-limited design.

The second example is one thick lens design with magnification $m = -3$, f-number equal to 2.5, object distance $l = -60$ mm, the shape factor of −0.38, and commercial glass BK7. The image distance is $l' = ml = 180$ mm, focal length $f = ll'/(l - l') = 45$ mm and lens diameter $D = f/f$-number= 18 mm. Following the methodology developed in the first example, we have the radii of curvature for a thin lens $r_1 = 75.0179$ mm and $r_2 = -33.7036$ mm, with the heights $y_1 = y_2 = D/2 = 9$ mm, we compute the sagittas for spherical surfaces $z_1 = 0.5558$ mm and $z_2 = -1.2564$ mm, respectively. Considering a lens edge thickness $e = 6$ mm, we have an axial thickness $d_1 = 7.8122$ mm and radii of curvatures $r_1 = 73.1455$ mm and $r_2 = -32.8624$ mm for a thick lens. The object and image positions concerning the vertices of the first and second surfaces are equal to $d_0 = l + H_1 = -56.3551$ mm

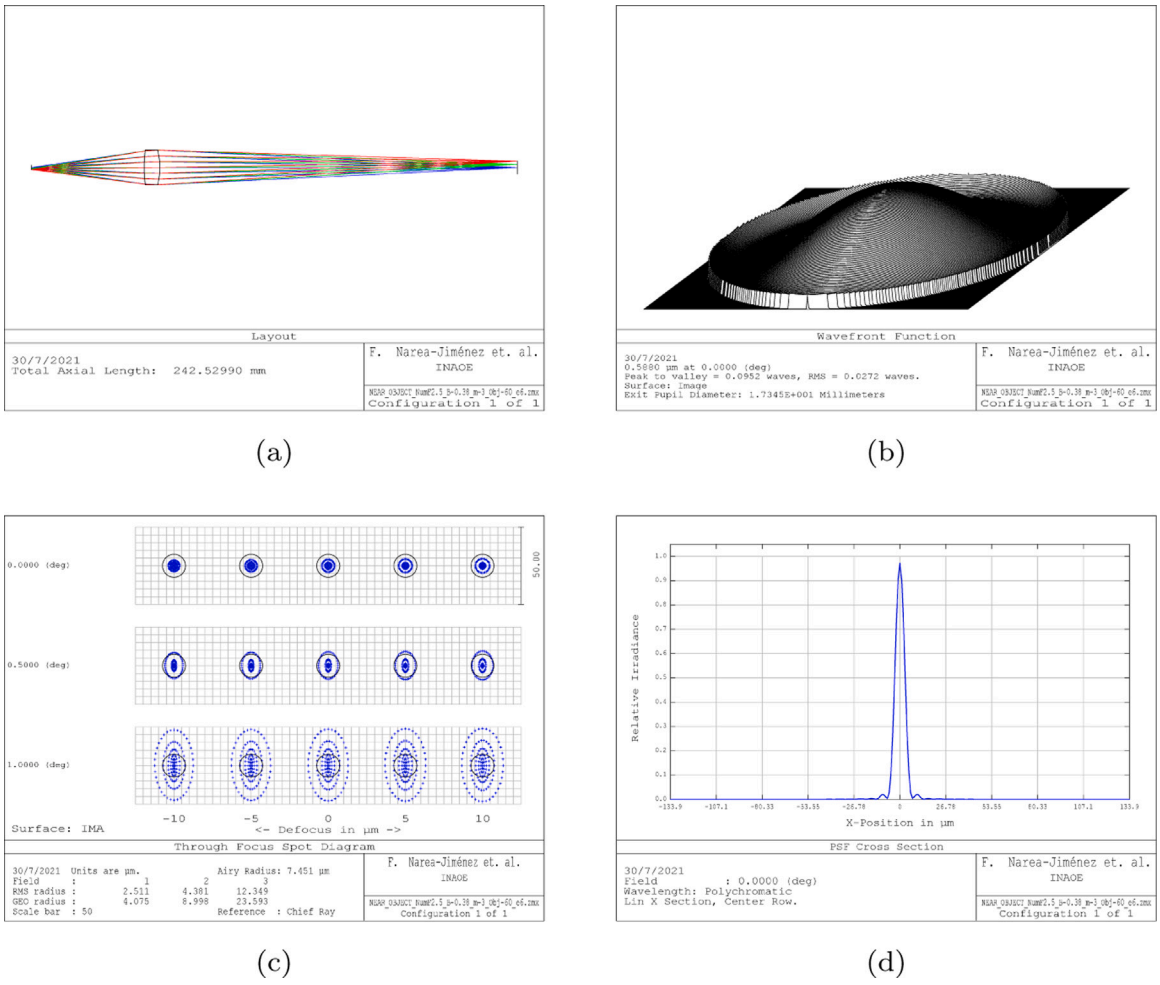

Fig. 4. Design case of a finite conjugate singlet.

and $d_2 = l' + H_2 = 178.3624$ mm, where $H_1 = 3.6448$ mm and $H_2 = -1.6375$ mm are the positions of the principal planes [24]. All first-order parameters calculate and show in Table 2. We choose the best solution for $z_1 = 0.5392$ mm that satisfies Eq. (27), and allow us to calculate director cosines of the refracted ray $L_1 = 0$, $M_1 = 0.0624$, and $N_1 = 0.9980$ between the conic surfaces, which are substituted in Eq. (26) to determine $D_1 = 5.9027$ mm this value uses to calculate the coordinates $y_2 = 9.3717$ mm and $z_2 = -1.3362$ mm. The first and second conic constants calculate by using the Eq. (12). These are equal to -8.2255 and -1.0012, respectively.

We obtain an aplanatic singlet with these values, as shown in Fig. 4(a), which illustrates the designed lens outline. Fig. 4(b) shows the wavefront with a peak-to-valley value of 0.0952λ and the RMS wavefront error of 0.0272λ. Fig. 4(c) shows residual spherical aberrations and astigmatism in the spot diagram. Fig. 4(d) shows the PSF, which shows a Strehl ratio of 0.9713. In the spot diagram of both examples, it is evident that the coma aberration is wholly corrected, unlike the results presented by Mikš [12], where this aberration is still apparent.

In both examples, we corroborate that Maréchal's criterion is satisfied in such a way that the method that we developed when performing this exact calculation using the equality of the optical path and the condition of Abbe's sine minimizes the RMS wavefront error [15,25]. Examples show wavefront correction at the center and on the edge of the lens, as we can see in 3(b) and 4(b). As shown 3(c) and 4(c) in the two examples for the field's margin, the spot diagram is like an ellipse showing astigmatism aberration.

We design other examples in different spectral regions with the developed method, such as the ultraviolet and infrared regions, which show our methodology's adequate functionality.

Conclusion

We calculate equations to obtain lenses free of spherical and coma aberration using third-order design and exact ray tracing, depending on the shape factor and the lenses' conic constants. Our third-order results are in agreement with the calculations made

by Kingslake and Shannon, among others. By making an exact ray tracing, we have eliminated the spherical and coma aberrations at the center and edge of the aperture, allow us to obtain a diffraction-limited system. We analyze cases, both for when the object is near or far from the lens. Our exact methodology is an alternative method of designing lenses that avoids using on-the-market optimization software.

It shows that the spot diagrams obtained are close to the diffraction limit. These results can be compared with any commercial optical design software when the conic constants are optimized, finding similar results. The examples presented exhibit the developed method's efficiency, particularly for f-number equal to or greater than 2.5 and minor fields of view, which agrees with Abbe, who proposed that aplanatism occurs near the center of the field. Strehl ratios are around 0.8 and RMS wavefront error $\leq \lambda/14$ obtain for any designed lens with the presented method, which shows that the coma and spherical aberration-corrected at any height of the incident marginal ray. The final optical design obtained with this method is ready to apply optical tolerance analysis.

Declaration of competing interest

The authors declare that they have no known competing financial interests or personal relationships that could have appeared to influence the work reported in this paper.

Acknowledgment

We appreciate the support from Consejo Nacional de Ciencia y Tecnología CONACYT-Mexico and Centro de Enseñanza Técnica Industrial CETI-Mexico.

References

[1] E. Conrady, Applied Optics and Optical Design, second ed., Dover Publications, 1992.
[2] R. Kingslake, R. Johnson, Lens Design Fundamentals, second ed., Elsevier Science, 2009.
[3] A. Jenkins, E. White, Fundamentals of Optics, fourth ed., McGraw-Hill, 1981.
[4] J. Castro-Ramos, M.T. Chavez-Garcia, S. Vazquez-Montiel, A. Cordero-Davila, Thick lenses free from spherical aberration designed by using exact ray tracing, in: Current Developments in Lens Design and Optical Engineering VI, vol. 5874, SPIE, 2005, pp. 270–280, http://dx.doi.org/10.1117/12.618078.
[5] B. Jurek, Optical Surfaces: Aspherical Optical Systems–X-Ray Optics–Reflecting Microscopes–Reflectors–Measurements, Elsevier Scientific Pub. Co. ; distribution for the U.S.A. and Canada, American Elsevier Pub. Co, Amsterdam, New York, 1977.
[6] M. Avendaño-Alejo, E. Román-Hernández, L. Castañeda, I. Moreno-Oliva, Analytic conic constants to reduce the spherical aberration of a single lens used in collimated light, Appl. Opt. 56 (22) (2017) 6244–6254, http://dx.doi.org/10.1364/AO.56.006244.
[7] C. Chen, Variations of spherical aberration and central coma of conceptual thin lenses, Appl. Opt. 55 (36) (2016) 10363–10369, http://dx.doi.org/10.1364/AO.55.010363.
[8] K. Slawomir, N. Jerzy, Z. Marek, Aplanatic correction of a hybrid lens, in: J.M. Sasian (Ed.), Novel Optical Systems Design and Optimization, vol. 2537, SPIE, International Society for Optics and Photonics, 1995, pp. 321–328, http://dx.doi.org/10.1117/12.216396.
[9] M. Zhang, D. Zhi, Y. Ma, P. Ma, R. Su, J. Wu, P. Zhou, L. Si, Coherent fiber-optics-array collimator based on a single unitary collimating lens: proposal design and experimental verification, Appl. Opt. 58 (6) (2019) 1491–1495, http://dx.doi.org/10.1364/AO.58.001491.
[10] S. Masato, Considering the pupil coordinate of aberration theory from the view point of the sine condition in the presence of spherical aberration, in: J.-L.M. Tissot, J.M. Raynor, L. Mazuray, R. Wartmann, A. Wood (Eds.), Optical Design and Engineering IV, vol. 8167, SPIE, International Society for Optics and Photonics, 2011, pp. 42–56, http://dx.doi.org/10.1117/12.896768.
[11] R.G. González-Acuña, H.A. Chaparro-Romo, J.C. Gutiérrez-Vega, Exact equations for stigmatic singlet design meeting the Abbe sine condition, Opt. Commun. 479 (2021) 21264152, http://dx.doi.org/10.1016/j.optcom.2020.126415.
[12] A. Mikš, P. Pokorný, Calculation of a lens system with one or two aspherical surfaces having corrected spherical aberration, J. Opt. Soc. Amer. A 37 (9) (2020) 1390–1397, http://dx.doi.org/10.1364/JOSAA.399361.
[13] M. Born, E. Wolf, Principles of Optics: Electromagnetic Theory of Propagation, Interference and Diffraction of Light, sixth ed., Pergamon Press, Oxford ; New York, 1980.
[14] S. Srivastava, V. Vasavada, V. Vasavada, S. Vasavada, M.R. Praveen, R. Reddy, A.R. Vasavada, Comparison of ocular wavefront aberrations in subluxated lenses before and after lens extraction with intraocular lens implantation, J. Cataract Refract. Surg. 44 (3) (2018) 336–340, http://dx.doi.org/10.1016/j.jcrs.2017.12.017.
[15] T. Welford, Aberrations of Optical Systems, A. Hilger, Great Britain, 1991.
[16] D. Malacara, Z. Malacara, Handbook of Optical Design, third ed., in: Optical science and engineering, CRC Press, Taylor & Francis, Boca Raton, FL, 2013.
[17] R. Shannon, The Art and Science of Optical Design, Camb. University Press, 1997.
[18] A. Mikš, J. Novák, Third-order aberration coefficients of a thick lens, Appl. Opt. 51 (33) (2012) 7883–7886, http://dx.doi.org/10.1364/AO.51.007883.
[19] A. Mikš, J. Novák, Third-order aberration coefficients of a thick lens with a given value of its focal length, Appl. Opt. 57 (15) (2018) http://dx.doi.org/10.1364/AO.57.004263.
[20] E. Abbe, Beiträge zur Theorie des Mikroskops und der mikroskopischen Wahrnehmung, Arch. Mikrosk. Anat. 9 (1) (1873) 413–468, http://dx.doi.org/10.1007/BF02956173.
[21] M. Mansuripur, Abbe's Sine condition, Opt. Photonics News 9 (2) (1998) 56–60, http://dx.doi.org/10.1364/OPN.9.2.000056.
[22] T.T. Elazhary, P. Zhou, C. Zhao, J.H. Burge, Generalized sine condition, Appl. Opt. 54 (16) (2015) 5037–5049, http://dx.doi.org/10.1364/AO.54.005037.
[23] J.J.M. Braat, Abbe sine condition and related imaging conditions in geometrical optics, in: C.H.F. Velzel (Ed.), Fifth International Topical Meeting on Education and Training in Optics, vol. 3190, International Society for Optics and Photonics, SPIE, 1997, pp. 59–64, http://dx.doi.org/10.1117/12.294417.
[24] E. Hecht, Optics, fifth ed., Pearson Education, Inc, Boston, 2017, p. 249.
[25] A. Maréchal, Etude des effets combinés de la diffraction et des aberrations géométriques sur l'image d'un point lumineux, in: SER (Riom), Éditions de la Revue d'optique théorique et instrumentale, 1948.